Inorganica Chimica Acta 380 (2012) 372–377

Contents lists available at SciVerse ScienceDirect

Inorganica Chimica Acta

journal homepage: www.elsevier.com/locate/ica

Ordered arrangements of metal nanoparticles on alpha-cyclodextrin inclusion complexes by magnetron sputtering

L. Barrientos [a,*], P. Allende [a], C. Orellana [a], P. Jara [b]

[a] Departamento de Química, Facultad de Ciencias Básicas, Universidad Metropolitana de Ciencias de la Educación, Santiago, Chile
[b] Departamento de Química, Facultad de Ciencias, Universidad de Chile, Santiago, Chile

ARTICLE INFO

Article history:
Available online 20 October 2011

Young Investigator Award Special Issue

Keywords:
Supramolecular stabilization
Metal nanoparticles
Metal–guest interaction
Magnetron sputtering

ABSTRACT

An ordered self-assembly of copper, silver and gold nanoparticles onto crystal faces of α-cyclodextrin/1-octanethiol and 2α-cyclodextrin/1-octylamine inclusion complexes by means of physical vapor deposition (magnetron sputtering) has been achieved. The preferential deposition on the (001) plane of the supramolecular crystal occurs because the –SH and $–NH_2$ groups from the guest molecules found within the α-cyclodextrin protrude into that plane. These functional groups form a two-dimensional hexagonal lattice that interacts with the metal nanoparticles, arranging them in an ordered way.

1. Introduction

In the era of nanotechnology, where properties are dependent on the size of the structure, prodigious discoveries and applications in multiple areas of science suggest the importance of understanding a systems structure and its impact on material properties [1,2]. This great interest is based on the quantum states of these materials, which are size-dependent, leading to new physical and chemical properties that differ considerably from the solid and molecular state [2].

One of the most interesting materials in this area, are metallic nanoparticles, which have special optical (plasmon band) [3], electronic [4], catalytic properties [5,6] and relativistic effects [7], as well as their wide applications for nanostructured and biological technologies [8–12].

Metal nanoparticles (NPs) can be synthesized by both physical and chemical methods. However, chemical approaches such as chemical reduction, electrochemical techniques, and photochemical reduction have been the most used [13,14]. Some reports have shown that the size, morphology, stability and properties of metal nanoparticles are strongly influenced by the experimental conditions, the kinetics with reducing agents, and the adsorption processes [15]. Therefore, the design of synthetic methods in which the size, morphology, stability and properties are controlled has become a major topic of interest [16,17].

In this sense, another preparation method, known as magnetron sputtering, presents several advantages. Basically, it consists in the sputtering of a high-purity metal target with argon ions, followed by the subsequent deposition of the sputtered metal atoms on the surface of a powder support material to create a uniform dispersion of nanoparticles [18]. As mentioned, this technique has several advantages over existing preparation methods. For example, there is no contamination from solvent or precursor molecules on the surface, the process is environmentally friendly, and there is no liquid waste.

Gold (AuNPs), silver (AgNPs) and copper nanoparticles (CuNPs) have been used in areas such as photography, catalysis, biological labeling, photonics, optoelectronics and surface-enhanced Raman scattering detection and nanomedicine, amount others [19–21].

To improve the study of materials properties at the nanoscale, an ordered arrangement of these systems is required. Many techniques have been developed for directing the self-assembly of nanoparticles into ordered aggregates [22–25]. Ghosh and Pal [26] reported that the self-assembly of nanoparticles has been of high interest to science, because it provides effective building blocks for physical, chemical, and biological applications. These assemblies present exciting possibilities as inter-particle separation, particle size, and particle stoichiometry may be individually manipulated to produce macroscopic solids [26]. An interesting and alternative arrangement is possible to obtain when using self-assembled structures through molecular recognition phenomena such as AuNPs onto α-cyclodextrin (α-CD) inclusion complexes [27].

Several possible processes exist when the cyclodextrins molecules (CDs) interact to form supramolecular assemblies [28]. The specific mechanism and corresponding driving force involved in the complex formation, as well factors responsible for their

* Corresponding author. Tel.: +56 2 2412495.
E-mail address: lorena.barrientos@umce.cl (L. Barrientos).

0020-1693/$ - see front matter © 2011 Elsevier B.V. All rights reserved.
doi:10.1016/j.ica.2011.10.032

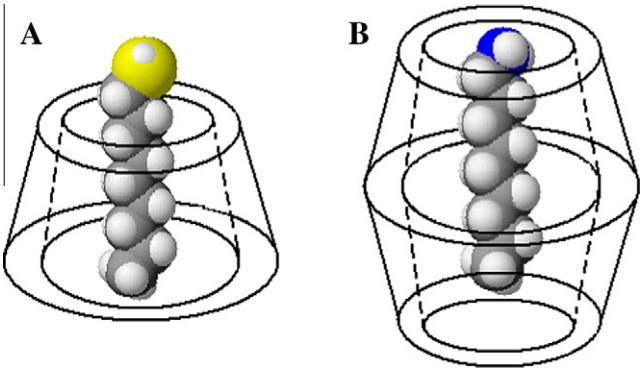

Fig. 1. Schematic representation of α-CD/$C_8H_{17}SH$ (A) and 2α-CD/$C_8H_{17}NH_2$ (B).

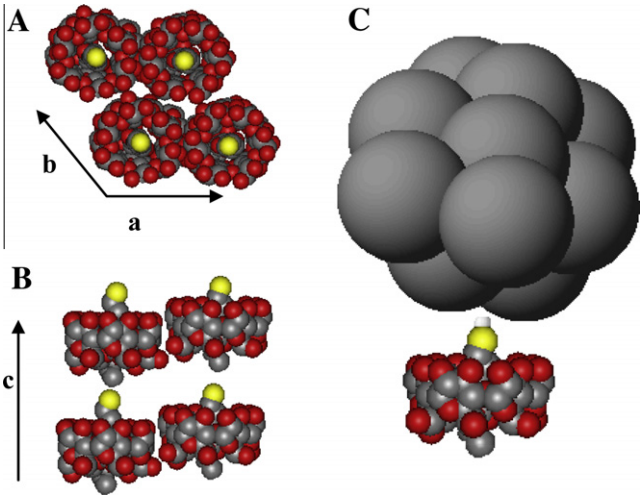

Fig. 2. Crystal packing diagram of hexagonal form of (001) face viewed from the crystallographic *c* axis (A) and the (100) face viewed from the crystallographic *a* axis (B), H atoms are not shown. Schematic representation of α-CD/$C_8H_{17}SH$ interacting with metal nanoparticle (C).

stability, become a problem of great interest. In order to understand this mechanism and explore potential applications, the ordered arrangement of nanoparticles has become an area of great interest. Creating an ordered arrangement requires a controlled self-assembly, for example as polymer surfaces [29], inorganic substrates [30–32] and single atomic monolayers [33,34]. Sada and co-workers [35] showed the first example of an anisotropic decoration of AuNPs onto a L-cystine single crystal. Further, we reported an ordered hexagonal arrangement of AuNPs, controlled by self-assembly on thiol groups of guest molecules embedded in supramolecular structure [27]. Thus, crystals provide a convenient way to preserve nanoparticles in the solid state without aggregation.

For instance, Reinhoudt and co-workers [36] reported the assembly of network aggregates from β-CD capped AuNPs and

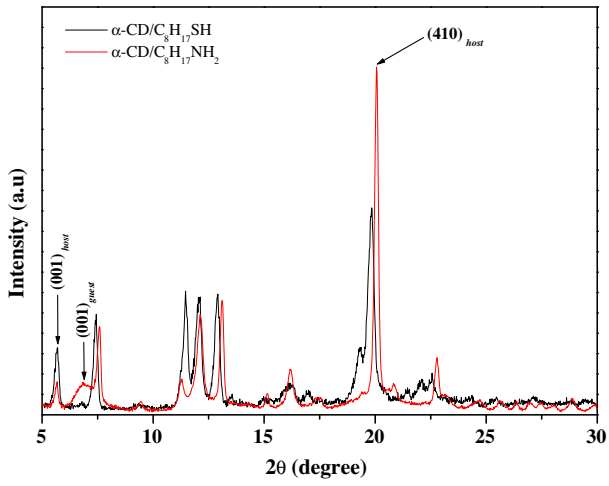

Fig. 3. Powder X-ray diffractogram of the α-CD host in the inclusion compounds at 295 K.

various adamantyl-containing guest molecules. Sortino and co-workers [37] showed a reversibly photoswitch by utilizing the self-assembly process of α-CD/azobenzene inclusion complex on AuNPs. Finally, Monflier and co-workers [38] reported the preparation of ruthenium nanoparticles stabilized by inclusion complexes formed between the chloride salt of *N*,*N*-dimethyl,*N*-hexadecyl,*N*-(2-hydroxyethyl)-ammonium and randomly methylated cyclodextrins.

To date no major effort has been reported to investigate cyclodextrins inclusion complexes that interact in an ordered way with metal nanoparticles such as silver, gold and copper. This order is possible to obtain by the magnetron sputtering technique, which generates a hetero-epitaxial growing of the nanoparticles onto the preferential crystal plane of the inclusion complex.

Therefore, it is interesting to study the order of particles and their interaction with a guest molecule by functional groups as thiol and amine that are outside of the supramolecular host. Here, as an alternative and even more versatile concept, we introduce in this work ordered arrangements of CuNPs, AgNPs and AuNPs produced by magnetron sputtering deposition onto α-cyclodextrin/1-octylamine (2α-CD/$C_8H_{17}NH_2$) and α-cyclodextrin/1-octanethiol (α-CD/$C_8H_{17}SH$). The guest molecules, specifically –NH_2 and –SH functional groups, form a two-dimensional hexagonal lattice that interacts with metal nanoparticles, arranging them in an ordered way.

2. Experimental

2.1. Chemicals and starting materials

All reagents and solvents used in this study were commercially available from Sigma–Aldrich Chemical Company and were used without further purification. The preferential deposition of metal

Table 1
Comparison of unit cell parameters of hexagonal phases.

Phase	$a = b$ (Å)	c (Å)	V (Å)	Metal/metal oxide *hkl*
α-CD/$C_8H_{17}SH$	23.78(14)	15.93(11)	7804.31	
2α-CD/$C_8H_{17}NH_2$	23.50 (9)	15.98 (7)	7645.80	
α-CD/$C_8H_{17}SH$/AuNPs	23.94 (8)	16.13 (6)	8007.72	$(111)_{Au}$, $(200)_{Au}$, $(220)_{Au}$, $(311)_{Au}$
α-CD/$C_8H_{17}SH$/Ag-Ag_2ONPs	23.78 (3)	16.05 (3)	7862.20	$(111)_{Ag}$, $(200)_{Ag}$
2α-CD/$C_8H_{17}NH_2$/Cu-CuONPs	23.65 (9)	15.99 (7)	7728.13	$(200)_{Cu}$, $(220)_{Cu}$, $(220)_{CuO}$, $(210)_{CuO}$

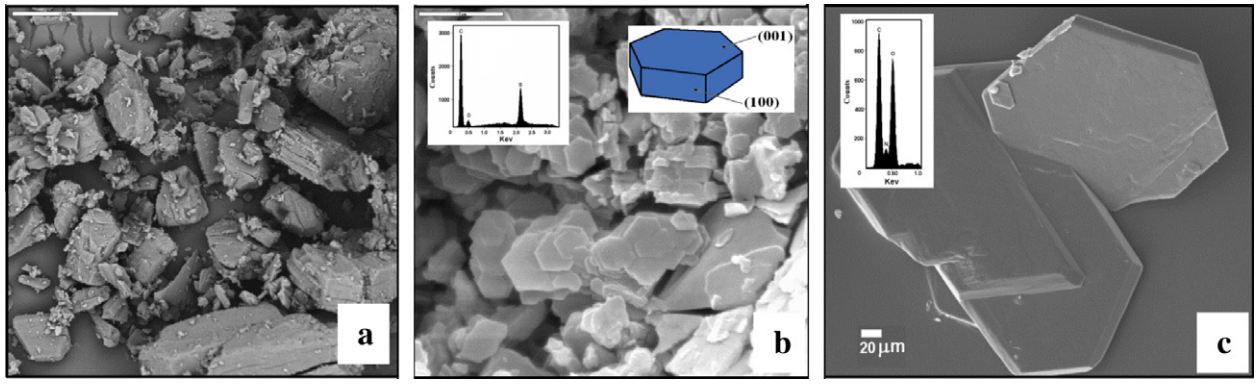

Fig. 4. SEM micrographies of α-CD pure (A), α-CD/$C_8H_{17}SH$ crystals (B) and α-CD/$C_8H_{17}NH_2$ crystals (C). Inserted in the Fig. 2B and C are the energy dispersive spectroscopy (EDS) spectra of the studied inclusion complexes.

nanoparticles was carried out by magnetron sputtering technique. The cathodes used were of electrolytic grade (99.99% purity).

2.2. Synthesis of α-cyclodextrin inclusion complexes

The synthesis of the inclusion complex was based on previously reported method for α-CD/$C_8H_{17}SH$ [39]. Specifically, supramolecular complexes were obtained by the reaction of 0.27 mL 1-octanotiol ($C_8H_{17}SH$) or 0.25 mL 1-octylamine ($C_8H_{17}NH_2$) and 10 mL of α-CD. The resulting white suspension was allowed to react for 24 h. The obtained microcrystals were filtered and washed with small amounts of water and acetone or methanol for α-CD/$C_8H_{17}SH$ and 2α-CD/$C_8H_{17}NH_2$ respectively. Yields: α-CD/$C_8H_{17}SH$ (97.2%), 2α-CD/$C_8H_{17}NH_2$ (85.6%).

2.3. Synthesis of metal nanoparticles

Microcrystals of inclusion complexes were dispersed inside of the magnetron sputtering chamber (magnetron sputter coater PELCO SC-6) to form a homogeneous layer prior to sputtering. The Cu, Ag or Au was deposited onto the substrate in an inert atmosphere (Ar) at room temperature. Vacuum: 1×10^{-5} atm; Current: 25 mA; exposure time: 60 s (Cu), 40 s (Ag) and 25 s (Au).

2.4. Characterization techniques

^{1}H-Nuclear Magnetic Resonance spectra were obtained at room temperature on an Advance 400 spectrometer in d_6-DMSO. Powder X-ray Diffraction (PXRD) data were collected at room temperature on a Siemens D 5000 powder diffractometer, with Cu Kα radiation in the range $2° < 2\theta < 80°$ (40 kV, 30 mA) and a graphite monochromator (λ = 1.540598 Å). Inclusion compounds and those that interacted with the nanoparticles, were ground to a fine powder in order to reduce the likelihood of the crystallites exhibiting a preferred orientation. The lattice parameters and refinement were calculated by the ITO method, which is the basis of the theoretical powder X-ray computer program. The two inclusion complexes peaks can be indexed as a hexagonal lattice (6/mmm) whose parameters are: $a = b \approx 23.7$ Å, $c \approx 15.9$ Å, $\alpha = \beta = 90°$ and $\gamma = 120°$ for α-CD.

Diffuse Reflectance spectra were obtained on a Shimadzu UV-3101 spectrophotometer. These spectra were transformed to absorbance through the Kubelka–Munk equation. Scanning electron microscopy (SEM) and Energy-Dispersive X-ray Spectroscopy (EDS) were performed on a LEO 1420 VP and Oxford Instruments EDS 7424 at 25 kV for inclusion complexes and 5 kV when these interact with metal nanoparticles. High-resolution Transmission electron microscopy (HRTEM) and electron diffraction (ED) were performed using a JEOL 2000FX microscope at 200 kV. For these analyses, the samples were deposited on a graphite/copper grid. Moreover, the average particle diameter (D) and the standard deviation (σ were calculated. Raman Spectra were recorded with a Renishaw Raman RM1000 equipped with a 514.5 nm laser line and electrically refrigerated CCD camera. Measurements were made at room temperature on solids samples.

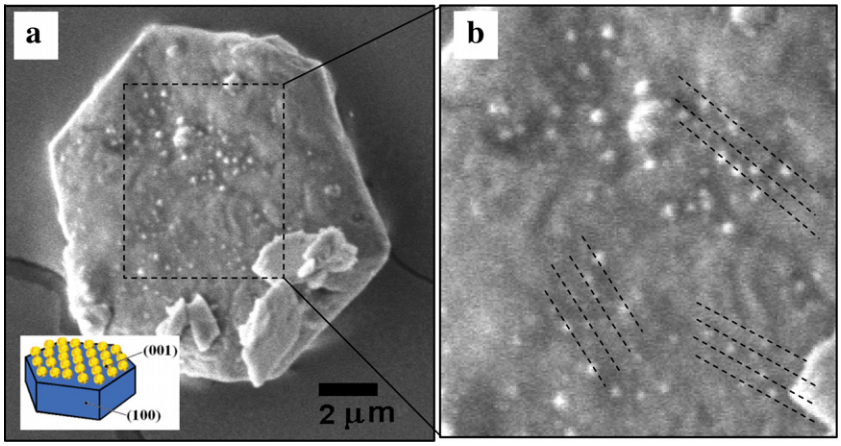

Fig. 5. SEM image of selective deposition of metal nanoparticles onto (001) crystal plane of α-CD/$C_8H_{17}NH_2$ (a). Magnification of the previous image showing the arrangements of metal nanoparticles (black lines) (b).

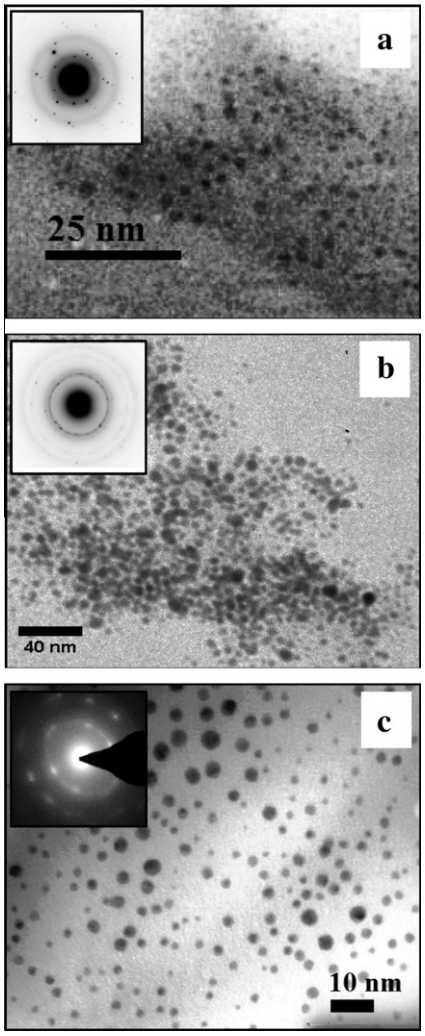

Fig. 6. TEM images of ordered arrangements of copper nanoparticles (A), silver nanoparticles (B) and gold nanoparticles (C). Insert in the figures are electron diffraction spots of the metal nanoparticles.

3. Results and discussion

3.1. ^{1}H-Nuclear Magnetic Resonance

NMR spectroscopy is one of the most efficient experimental techniques to investigate molecular interactions [40]. This technique allows observing chemical shifts of host and guest species and therefore the formation and stoichiometry of an inclusion complex. The host–guest ratio observed was 2:1 for 2α-CD/$C_8H_{17}NH_2$ and 1:1 for α-CD/$C_8H_{17}SH$. This stoichiometry was determined considering as reference the chemical shift of $-CH_3$ group (0.8 ppm) of the guests. The spectra show the characteristic signs of the guests to high fields (0.8–2.5 ppm), generating new chemical shifts and splitting with respect to pure compounds. On the other hand, the chemical shifts of the α-CD (3–5.5 ppm) allow determine the host number per guest. Fig. 1 shows a schematic representation of the corresponding inclusion complexes. This difference is attributed to the hydrophilic character of the –SH group, "forcing" the guest molecule to move outside of α-CD cavity, with greater freedom than the $-NH_2$ group that has a lower hydrophilic character (NMR spectra are show in Fig. S1 in Supplementary material). As a consequence, there is a higher interaction between $-NH_2$ and the α-CD host, leaving the aliphatic chain inside the cavity and forming a 2:1 complex.

3.2. Powder X-ray diffraction

The cell parameters and Miller indices (see Table S2 in Supplementary material) of hexagonal microcrystals were determined by powder X-ray diffraction studies. The values of the (a) and (b) cell units obtained for these complexes, do not agree with those reported for similar guests [27], including dialkylamines [41–43]. However, the dimensions of the *a* and *b* axes obtained by us, were similar to those reported in the α-CD/cyclopentanone complex, whose structure was elucidated by neutron diffraction [44] and with the values obtained for the single crystal structure of the α-CD/octanoic acid complex [45]. The molecular packing diagrams are shown in Fig. 2.

The observed and calculated interplanar spacing of the host lattice (d_{hkl}) and the unit cell parameters are displayed in Table S1 in Supplementary material and Table 1, respectively. These features correspond to a 2D array of hexagonal channels along which the translation repeat unit *c* of about 16 Å, which is always the same regardless of the guest nature, agreeing with the basic host structure observed for α-CD inclusion compounds.

The diffractograms in Fig. 3 shows that in addition to the peaks of the host structure, one peak corresponding to the guest reflection may be identified: $2\theta = 7.03$ (12.57 Å) for 2α-CD/$C_8H_{17}NH_2$ and $2\theta = 6.80$ ($d = 12.97$ Å) for α-CD/$C_8H_{17}SH$, both of which were reported previously by our group [46].

The space periodicity of the guest species along the channels, can be unequivocally obtained for both complexes. The corresponding values are comparable with the length of the guest molecules in their most extended linear conformation ($C_8H_{17}NH_2$: 11.07 Å and $C_8H_{17}SH$: 11.68 Å). The interaction with metal nanoparticles was also studied. Interestingly, the peaks related to the guest molecules in Fig. 3 disappear when the guest is interacting with Cu, Ag or Au NPs due to guest's disorder, with loss of periodicity. This disorder is a consequence of the guest displacement, inside of the α-CD cavity, when –SH or $-NH_2$ groups are interacting with the NPs.

The guest displacement was evidenced by an increase in the lattice parameters (see Table 1), especially the *c*-axis (increase from 15.93 to 16.13 Å) in α-CD/$C_8H_{17}SH$/AuNPs. As mentioned, the NPs induce a shift of the guest molecule, forcing it to leave the (001) plane and generating this increase. On the other hand, PXRD analysis of α-CD inclusion complexes and metal NPs confirms that the structure of the supramolecular crystal matrix remains unchanged. The diffractograms show additional diffraction lines attributed to metal and metal oxide phases that are presented in Table 1.

3.3. Scanning electron microscopy

Fig. 4 shows the SEM images of hexagonal micrometer-sized single crystals, which reveals well-defined shapes with sharp edges. The crystal faces could be easily assigned by the hexagonal

Table 2
Diameter (D), standard deviation (σ) and electron diffraction pattern (ED) of metal particles recorded by transmission electron microscopy.

Phases	D (nm)	σ (nm)	ED
α-CD/$C_8H_{17}SH$/AuNPs	2.33	0.72	(111), (200), (220), (311)
2α-CD/$C_8H_{17}NH_2$/Cu-CuONPs	2.01	0.92	(200)Cu, (220)Cu, (220)CuO, (200)CuO, (111)CuO
α-CD/$C_8H_{17}SH$/Ag-Ag_2ONPs	3.65	2.5	(111)Ag, (200) Ag, (110) Ag_2O (211) Ag_2O

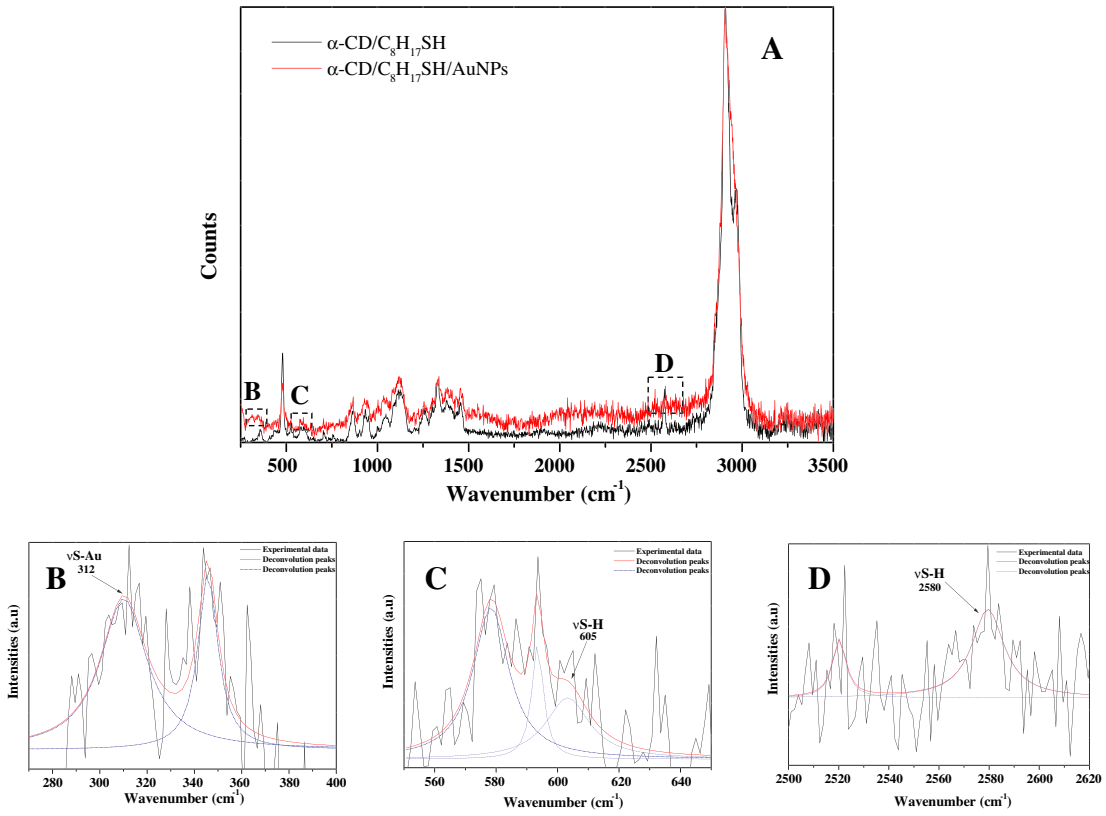

Fig. 7. Raman spectra of studied systems. Raman spectrum of α-CD/$C_8H_{17}SH$ and α-CD/$C_8H_{17}SH$/AuNPs (A), Stretching band of gold–sulphur at 312 cm^{-1} (B), bending band of thiol group interacting with gold at 605 cm^{-1} (C) and stretching band of thiol group interacting with gold at 2580 cm^{-1} (D).

package and the results obtained by PXRD. Moreover, SEM images show a morphological change from pure α-CD to α-CD/$C_8H_{17}SH$ or α-CD/$C_8H_{17}NH_2$ crystals. In addition, EDS spectra inserted in Fig. 4 demonstrate the chemical composition of the inclusion complexes.

To investigate the face-selective adhesion of nanoparticles on (001) crystal planes by electron microscopy, decorating experiments on micrometer-sized crystals were carried out, and were analyzed by SEM. Interestingly, nanoparticle deposition was observed only on hexagonal surfaces while the rectangular faces remained smooth (see Fig. 5). The hexagonal faces were assigned to crystallographic (*00l*) faces and the rectangular faces were assigned to (*h00*) and (*0k0*) faces, and so on. These results indicates that metal NPs selectively interacted with the (001) faces.

Therefore, in the crystal structure the supramolecular complexes are arranged in channel structures through two dimensional networks between guest molecules and α-CD hosts. The α-CD network runs parallel to the hexagonal faces, and the –SH or $–NH_2$ groups are exposed on the surface of the (001) hexagonal face. These groups have the possibility to interact with metal NPs through self-assembly processes.

3.4. High-resolution transmission electron microscopy

The hetero-epitaxial growth of metal nanoparticles onto (001) crystal face, where the –SH or $–NH_2$ groups are exposed outside the α-CD cavity, has been analyzed by TEM. Several linear metal arrangements were observed, leading to hexagonal ordering in some areas (~40%). TEM shows an inter-nanoparticle spacing of 50 Å for AuNPs and CuNPs and 100 Å for AgNPs, twice the CD unit's distance for gold and copper, and four units for silver, indicating that the NPs are located in alternated form on α-CD hosts (see Fig. 6). These distances correspond to the guests distance and are proportional to lattice parameters found by PXRD, confirming that the metal NPs grow on –SH or $–NH_2$ sites. Moreover, the AuNPs stabilized by α-ciclodextrin/dodecanethiol (α-CD/$C_{12}H_{25}SH$) [25] and α-CD/$C_8H_{17}SH$ were compared. We can see that the dodecanethiol guest stabilizes a higher percentage of hexagonal particles than the octanethiol. However, the particles size and distribution of them are similar. This behavior could be related to the stoichiometry of these systems, where the α-CD/$C_8H_{17}SH$ complex shows a 1:1 (host:guest) and α-CD/$C_{12}H_{25}SH$ was 2:1. This ratio could suggest that the 2:1 systems are the best complexes to stabilize the nanoparticles in an ordered way.

The phenomenon of site-selective nanoparticles growth is called "hetero-epitaxial growth", because the particles immobilization is due to interaction of free-dangling –SH or $–NH_2$ groups with the metal. This leads to the stabilization of particles on the crystalline surface. Therefore, the crystal provides a convenient way of storing the NPs in the solid state without aggregation.

The diffraction patterns showed in Fig. 6 and analyzed in Table 2 confirmed the presence of Au, Cu and Ag with the corresponding planes for fcc metal phase and some patterns for oxide phases in Ag and Cu.

3.5. Surface plasmon resonance (SPR)

The metal NPs on inclusion complexes show the SPR with a maximum absorption around 531, 456 and 242 nm for Au, Ag and Cu NPs respectively. The plasmon band observed (see Fig. S2 in Supplementary material) is shifted to longer wavelengths and extremely broadened.

The sputter time of inclusion complexes was determinate by UV–Vis absorption spectroscopy. The exposure times were 60, 40 and 25 s for Cu, Ag and Au, respectively. These exposure times were necessary to synthesize small particles without aggregation.

The broadening, together with the red-shift of the plasmon band, can be assigned to a dipolar coupling between neighboring particles and to a change of dielectric environment. Goettmann and Moores [47] mentioned the importance of the dielectric environment on the surface plasmon band position. If the distances between AuNPs are around 3 and 7 nm, the plasmon band appears at 555 and 530 nm, respectively. This generates a shift to longer wavelengths in regard to the typical plasmon bands of colloids at 520 nm. In this way, the results permit to estimate by SPR the inter-particle distance in the gold case as approximately 5 nm. These values are in accordance with the inter-particle distance obtained by TEM.

3.6. Raman spectroscopy

Fig. 7 shows the Raman spectra of α-CD/$C_8H_{17}SH$ and α-CD/$C_8H_{17}SH$/AuNPs. The spectra show the three Raman bands related with the guest–metal interaction. Specifically, the interactions between S–H and Au were studied. The signal appearing at 312 cm^{-1} was assigned to the Au–S stretching, while the one at 605 cm^{-1}, was related to the bending band of S–H group interacting with gold. Finally, the S–H stretching peak appeared at 2575 cm^{-1}, reflecting the interaction of this group with Au.

The Raman studies confirm that the self-assembly of metal particles were mediated by functional groups such as –SH and $–NH_2$, generating a hetero-epitaxial growth [2] of nanoparticles by intermolecular interaction. This interaction is between the sulphur or nitrogen of the guest and metal, which permit the metal nanoparticles stabilization.

4. Conclusions

In conclusion, the self-assembly by magnetron sputtering of copper, silver and gold nanoparticles onto microcrystal faces of α-CD/$C_8H_{17}SH$ and α-CD/$C_8H_{17}NH_2$ was achieved. Preferential deposition on the (0 0 1) plane of the α-CD inclusion complex crystal occurs because the –SH or $–NH_2$ groups from the guest molecules found within the α-CD protrude into this plane. These groups form a two dimensional hexagonal lattice that interacts with metal nanoparticles, stabilizing and arranging them in an ordered way.

The magnetron sputtering technique used to prepare ordered metal nanoparticles has several advantages, such as the lack of waste stream and scalability that make it attractive for industrial applications. This work gives the first evidence of metal nanoparticles assemblies mediated by a guest molecule in a supramolecular structure. The variation of surfactant guest and metal nanoparticles should provide various composite materials coated by self-assembled nanoparticles.

Acknowledgements

This research was possible thanks to financial support of FONDECYT, Grant Nos. 3100088 and 1080505. The authors thank Maria Concepción Gutierrez and Francisco del Monte for the TEM studies at ICMM-CSIC, Spain.

Appendix A. Supplementary material

Supplementary data associated with this article can be found, in the online version, at doi:10.1016/j.ica.2011.10.032.

References

[1] N. Ekekwe (Ed.), Nanotechnology and Microelectronics: Global Diffusion, Economics and Policy, Information Science Reference IGI Global, New York, 2010.
[2] C. Poole Jr., F. Owens, Introduction of Nanotechnology, John Wiley & Sons, 2003.
[3] N. Halas, S. Lal, W. Chang, S. Link, P. Nordlander, Chem. Rev. 111 (2011) 3913.
[4] R. Andres et al., Science 272 (1996) 1323.
[5] B. Du, O. Zaluzhna, Y. Tong, Phys. Chem. Chem. Phys. 13 (2011) 11568.
[6] D. Astruc, F. Lu, J. Ruiz-Aranzaes, Angew. Chem., Int. Ed. 44 (2005) 7852.
[7] X. Zhang, J. Kuo, M. Gu, X. Fan, P. Bai, Q. Song, C. Sun, Nanoscale 2 (2010) 412.
[8] A. Karttunen, M. Linnolahti, et al., Chem. Commun. (2008) 465.
[9] M.C. Daniel, D. Astruc, Chem. Rev. 104 (2004) 293.
[10] C. Teranishi, R. Chim. 6 (2003) 979.
[11] S. Link, M.A. El-Sayed, Int. Rev. Phys. Chem. 19 (2000) 409.
[12] M. Brust, C. Kiely, Colloids and Surfaces A: Physicochem. Eng. Aspects 202 (2002) 175.
[13] I. Capek, Adv. Colloid Interface Sci. 110 (2004) 49.
[14] M. Nakamoto, Y. Kashiwagi, M. Yamamoto, Inorg. Chim. Acta 358 (2005) 4229.
[15] A. Roucoux, J. Schulz, H. Patin, Chem. Rev. 102 (2002) 3757.
[16] B. Knoll, F. Keilmann, Nature (1999) 399.
[17] S. Sengupta, D. Eavarone, I. Capila, G. Zhao, N. Watson, T. Kiziltepe, et al., Nature (2005) 436.
[18] G. Veith, G.A. Lupini, S. Pennycook, S.W. Ownby, N. Dudney, J. Catal. 231 (2005) 151.
[19] V. Sharma et al., Adv. Colloid Interface Sci. 145 (2009) 83.
[20] A. Campion, P. Kambhampati, Chem. Soc. Rev. 27 (1998) 241.
[21] E. Boisselier, D. Astruc, Chem. Soc. Rev. 38 (2009) 1759.
[22] A. Badia, W. Gao, S. Singh, L. Demers, L. Cuccia, L. Reven, Langmuir 12 (1996) 1262.
[23] J. Spatz, A. Roescher, M. Moller, Adv. Mater. 8 (1996) 337.
[24] N. Kimizuka, T. Kunitake, Adv. Mater. 8 (1996) 89.
[25] L. Motte, F. Billoudet, M. Pileni, J. Phys. Chem. 99 (1995) 16425.
[26] S. Ghosh, T. Pal, Chem. Rev. 107 (2007) 4797.
[27] L. Barrientos, N. Yutronic, F. del Monte, M. Gutiérrez, P. Jara, New J. Chem. 31 (2007) 1400.
[28] E. Chernykh, S. Brichkin, High Energy Chem. 44 (2010) 83.
[29] R. Henhar, T. Norstern, V. Rotello, Adv. Mater. 17 (2005) 657.
[30] M. Murugesan, D. Cunningham, J.-L. Martinez-Albertos, R. Vrcelj, B. Moore, Chem. Commun. (2005) 2677.
[31] T. Shimizu, T. Teranishi, S. Hasegawa, M. Miyake, J. Phys. Chem. B. 107 (2003) 2719.
[32] L. Bardotti, B. Prevel, P. Jensen, M. Treilleux, P. Melinon, A. Perez, J. Gierak, G. Faini, D. Mailly, Appl. Surf. Sci. 191 (2002) 205.
[33] S. Zhang, L. Chandra, C. Gorman, J. Am. Chem. Soc. 129 (2007) 4876.
[34] L. Nagle, D. Ryan, S. Cobbe, D. Fitzmaurice, Nano Lett. 3 (2003) 51.
[35] Y. Fujiki, N. Tokunaga, S. Shinkai, K. Sada, Angew. Chem., Int. Ed. 45 (2006) 4764.
[36] O. Crespo-Biel, A. Jukovic, M. Karlsson, D. Reinhoudt, J. Huskens, Isr. J. Chem. 45 (2005) 353.
[37] F. Callari, S. Petralia, S. Sortino, Chem. Commun. (2006) 1009.
[38] C. Hubert, A. Denicourt-Nowicki, A. Roucoux, D. Landy, B. Leger, G. Crowyn, Eric Monflier, Chem. Commun. (2009) 1228.
[39] P. Jara, L. Barrientos, B. Herrera, I. Sobrados, J. Chil. Chem. Soc. 53 (2008) 1399.
[40] Chanketadze et al., J. Chromatogr. A. 798 (1998) 315.
[41] P. Jara, M. Justiniani, N. Yutronic, I. Sobrados, J. Inclusion Phenom. Mol. Recognit. Chem. 32 (1998) 1.
[42] K. Takeo, T. Kuge, Agr. Biol. Chem. 34 (1970) 1787.
[43] K. Takeo, T. Kuge, Agr. Biol. Chem. 36 (1972) 2615.
[44] Le. Bas, G. Mason, S. A. Acta Cryst. B 50 (1994) 717.
[45] S. Rodrıquez-Llamazarez, N. Yutronic, P. Jara, U. Englert, M. Noyong, U. Simon, Eur. J. Org. Chem. (2007) 4298.
[46] L. Barrientos, N. Yutronic, M. Muñoz, N. Silva, P. Jara, Supramol. Chem. 21 (2009) 264.
[47] A. Moores, F. Goettmann, New J. Chem. 30 (2006) 1121.